

UDC

TENSILE DEFORMATION INDUCED STRUCTURAL REARRANGEMENT IN AMORPHOUS SILICON NITRIDE© 2012 N. Liao^{1*}, W. Xue¹, P. Yang², M. Zhang¹¹College of Mechanical and Electrical Engineering, Wenzhou University, Wenzhou, 325035, P.R.China²Laboratory of Materials and Micro-Structural Integrity, Jiangsu University, Zhenjiang, P.R.China

Received October, 18, 2010

С доработки — January, 19, 2011

Silicon nitride exhibits good mechanical properties and thermal stability at high temperatures. Since experiments have limitations in nanoscale characterization of the chemical structure and related properties, atomistic simulation is a proper way to investigate the mechanism of this unique feature. In this paper, the melt-quench method is used to generate the amorphous structure of silicon nitride; then the structural properties of silicon nitride under tensile deformation were studied by angular pair distribution functions. The corresponding mechanism of tensile stress induced structure rearrangement is explored.

Key words: silicon nitride, molecular dynamics, tensile deformation, amorphous structure.

INTRODUCTION

Silicon nitride (Si_3N_4) is a hard ceramic with high wear resistance, low coefficient of thermal expansion and unusually high fracture toughness over a broad temperature range. These properties result in excellent thermal stability, which makes Si_3N_4 attractive for semiconductor applications, protective coatings, and X-ray mask materials [1]. However, the application of Si_3N_4 is restricted by its low fracture toughness. It becomes essential to understand the structural and mechanical properties of silicon nitride in order to control the film properties during fabrication. The initiation of a brittle fracture and the energy calculation of the process were addressed in the pioneering work based on continuum mechanics [2—4]. However, the crack path and changes in the structure during tensile deformation were not considered due to the limitations of continuum mechanics.

The molecular dynamics (MD) simulation is especially suitable for the simulation of the structural and mechanical properties of materials at the atomic scale. Soules [5] reported studies of sodium silicate glass under tension loading; they showed that atomic bonds were elastically stretched at the beginning, then plastic deformation occurred, and finally a flaw formed, which resulted in separation. The stress-strain curve presented a brittle fracture as the tensile stress dropped rapidly after reaching the ultimate stress. Simmons et al. [6, 7] studied the fracture process of vitreous silica with a uniaxial strain at different strain rates. They found that the glass strength increased with increasing strain rates, which was attributed to the fact that the sample has more time to relieve its strain by a structural rearrangement of atoms at lower strain rates. A PDF analysis was performed to investigate the structure of interfacial regions in the Si_3N_4 nanophase [8]; they found the second and the third peak of PDF for Si—N to be much broader, and there is a decrease in the nearest-neighbor coordination of Si atoms in the interfacial regions. However, despite all these investigations, to our best knowledge, the structural characteristics during tensile deformation were still not studied.

Our main interest is the tensile stress induced structural characteristics of Si_3N_4 . At first, the melt-quench method was used to generate the amorphous structure of silicon nitride. Then a tensile loading

* E-mail: ln55@163.com

was applied and the corresponding structural rearrangement were studied by PDF, structure factor and angular distribution.

METHODOLOGY

Molecular dynamics simulation requires the definition of a potential function for particle interactions in the simulation. The Tersoff potential [9] is a three-body potential function that includes an angular contribution of the force. It is widely used in various applications for silicon, carbon, SiC, and Si₃N₄, in which the angles between the atoms act as an important factor. We chose the Tersoff potential to simulate silicon nitride and the potential parameters of [10] were used. The N—N attractive item in the potential energy for Si₃N₄ and SiCN was turned off to avoid generating N₂ gas [11, 12]. The model contains 108843 atoms that correspond to a density of 3.5 g/cm³. The melt-quench technique is used to generate the amorphous structures of silicon nitride from random distributed atoms in the simulation box. To mimic the melt-quench process, the system is heated to a very high temperature in order to simulate melting and then is rapidly cooled down to room temperature. After some test simulations, the following procedure is proposed, which can generate structures with relatively low energy.

1) The system is heated to 8000 K by 20 ps of NVT simulation in order to make it jump out the local energy minimum.

2) Cool the system down to a secondary high temperature 3000 K for 10 ps.

3) Fix the system temperature at 3000 K for 500 ps.

4) Further cool the system down to room temperature for 2000 ps.

5) Equilibrate the system at room temperature for 10 ps.

Lammps codes [13] are used to conduct the simulations. The stress tensor for the atom *i* is given by the following formula, where a and b take on values *x*, *y*, *z* to generate the 6 components of the symmetric tensor [13]. The first term is a kinetic energy contribution for the atom *i*, the second term is a pairwise energy contribution where *n* loops over its neighbors. *r*₁/*r*₂ and *F*₁/*F*₂ are the positions and the forces of the two atoms resulting from the pairwise interaction. The third term to the sixth term are contributions of bond, angle, dihedral, and improper interactions which the atom *i* involves. The final term accounts for internal constraint forces applying to the atom *i*.

$$S_{ab} = - \left[mv_a v_b + \frac{1}{2} P_p + \frac{1}{2} P_b + \frac{1}{3} P_a + \frac{1}{4} P_d + \frac{1}{4} P_i + \sum_{n=1}^{N_f} r_{i_a} F_{i_b} \right] \quad (1)$$

$$P_p = \sum_{n=1}^{N_p} (r_{1a} F_{1b} + r_{2a} F_{2b}), \quad P_b = \sum_{n=1}^{N_b} (r_{1a} F_{1b} + r_{2a} F_{2b}), \quad P_a = \sum_{n=1}^{N_a} (r_{1a} F_{1b} + r_{2a} F_{2b} + r_{3a} F_{3b}),$$

$$P_d = \sum_{n=1}^{N_d} (r_{1a} F_{1b} + r_{2a} F_{2b} + r_{3a} F_{3b} + r_{4a} F_{4b}), \quad P_i = \sum_{n=1}^{N_i} (r_{1a} F_{1b} + r_{2a} F_{2b} + r_{3a} F_{3b} + r_{4a} F_{4b}).$$

The partial static structure factors are calculated to investigate the structure features on intermediate length scales. It is defined as [14]

$$S_{\alpha\beta}(q) = \frac{1}{N} \sum_{k=1}^{N_\alpha} \sum_{l=1}^{N_\beta} \langle \exp(iq \cdot r_{kl}) \rangle \quad \alpha, \beta = \text{Si, O} \quad (2)$$

where N_α is the number of atoms of the type α , q is the wave vector, and $r_{kl} = r_k - r_l$ is the distance vector between the particle k and particle l . Based on these partial static structure factors, the neutron static structure factors can be calculated as

$$S_n(q) = \frac{\sum_{\alpha,\beta} b_\alpha b_\beta (c_\alpha c_\beta)^{1/2} S_{\alpha\beta}(q)}{\left(\sum_{\alpha} b_\alpha c_\alpha \right)^2} \quad (3)$$

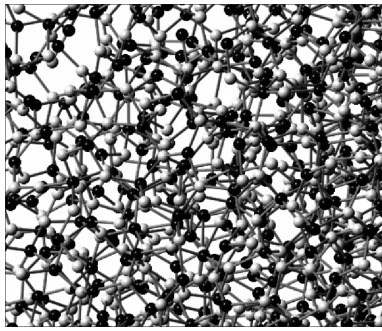


Fig. 1. Generated amorphous Si_3N_4 structure obtained by the melt quench method (Si and N atoms are presented in blue and white respectively)

where c_α and c_β are the concentration of α - and β -type atoms, and b_α and b_β are the coherent neutron scattering cross sections for α - and β -type atom nuclei.

RESULTS AND DISCUSSION

The generated a- Si_3N_4 structure is shown in Fig. 1, it can be observed that silicon atoms are bonded to nitrogen atoms and no N—N bond is present.

The atomic correlations are investigated by partial pair distribution functions (PDFs), which are shown in Fig. 2. As shown in Fig. 2, *a*, the Si—N bond length is determined by the sharp peak observed at $r_{\text{SiN}} = 1.75 \text{ \AA}$, which contributes to the first peak of the total correlation function. The second nearest neighbor distance for Si—Si is 2.9 \AA , which contributes to the third peak of the total correlation function. As expected, the calculated total PDF is also close to the experimental result [15]; the comparison of the simulation and experiment is shown in Fig. 2, *b*.

A tensile loading was applied by displacing the box in the z direction with a strain of 0.0025 for every 10 ps. In the following, the comparisons of the structural features for unstrained and strained Si_3N_4 are presented. From the PDF data it follows, as shown in Fig. 3, that the tensile stain results in a very short bond length present in the deformed structure, which is due to the compression in the x and y directions. And this also causes lower and broader peaks in the PDF of the strained structure.

Further information about the local structure is provided by the angular distribution, as shown in Fig. 4. The Si—N—Si distribution is narrow and shows a peak around 120° , which is in agreement with the peak at 121° in the experiments [16]. The N—Si—N distribution is wider than the above case; it ranges from 90° to 130° . Similarly to the PDF results, the angular distribution of the strained structure also presents lower and broader peaks. Meanwhile, the Si—N—Si and N—Si—N distributions show a trend to have smaller angles, while N—Si—Si and Si—N—N show an opposite trend.

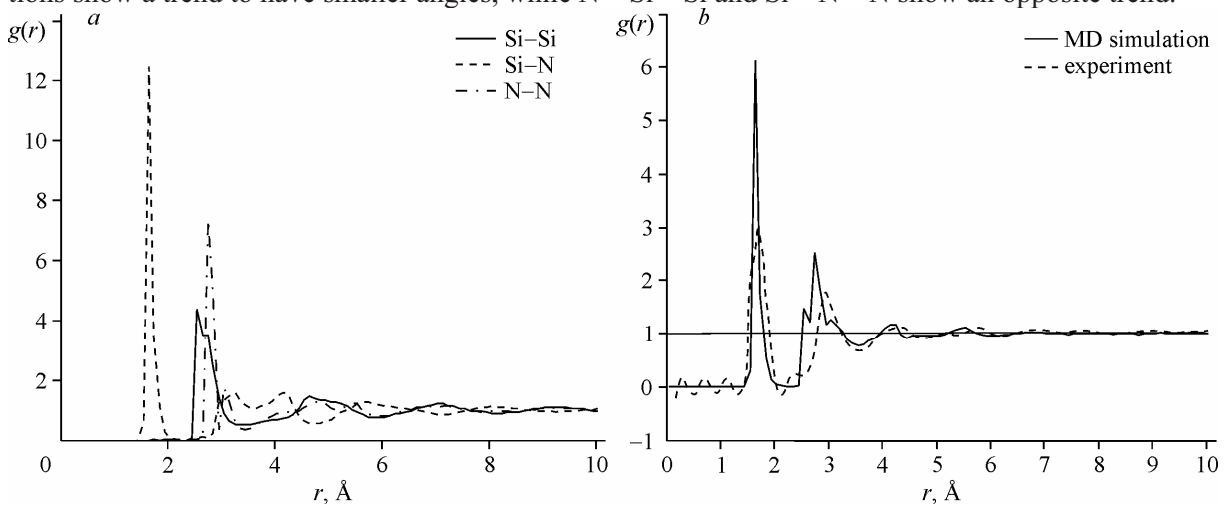


Fig. 2. Partial and total PDFs obtained by the MD simulation and compared with the experimental result [15]

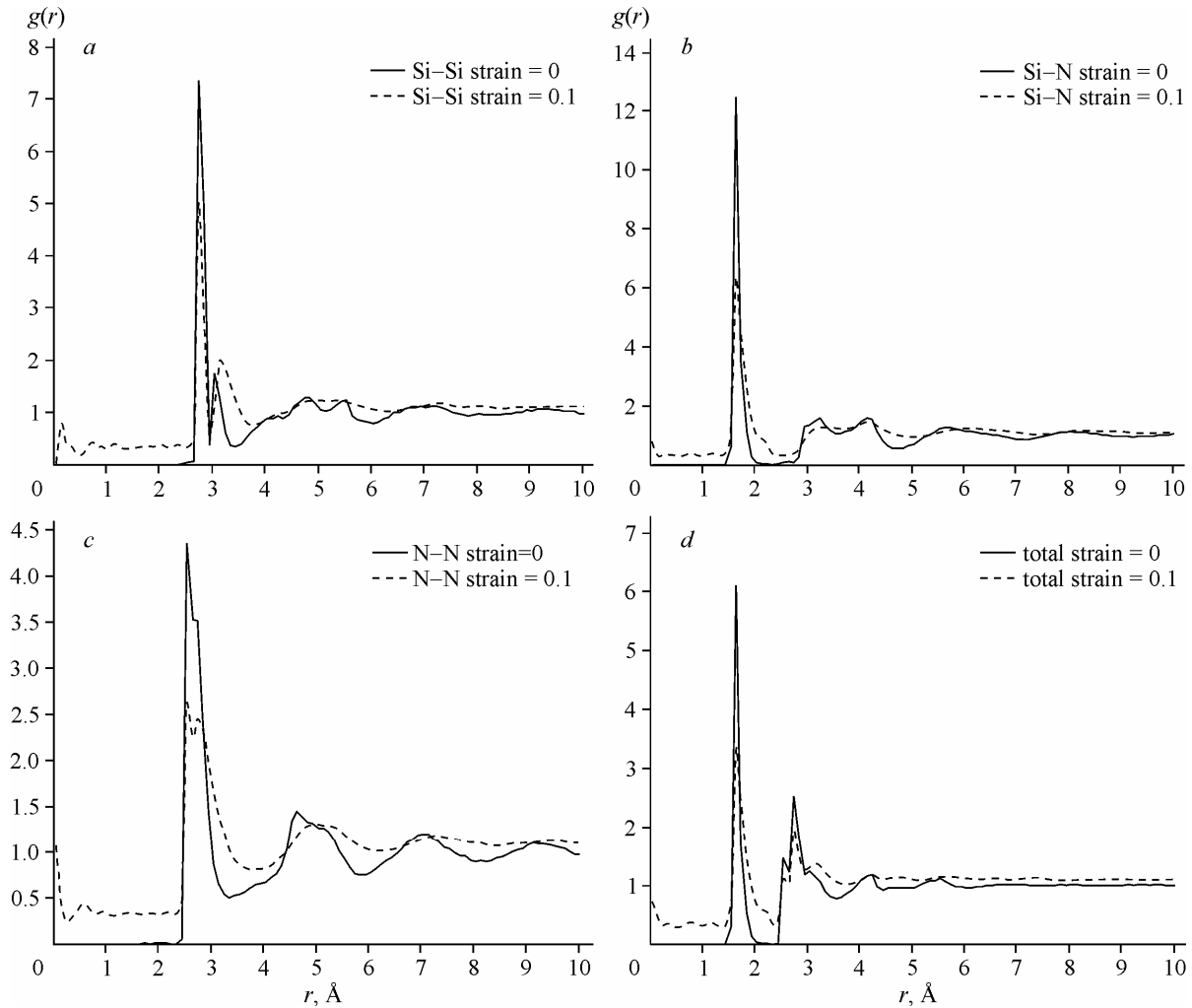


Fig. 3. Comparison on PDF results for unstrained and strained Si_3N_4

CONCLUSIONS

In this study, we applied the molecular dynamics simulation to study the structural characteristics of silicon nitride under tensile deformation. The melt-quench method was used to obtain the amorphous structures and the Tersoff potential was used for all the simulations. The simulation results show that the methodology used here can reproduce the important structural properties of a- Si_3N_4 . The comparison of the unstrained and strained structures shows that the deformed structure presents lower and broader peaks in the PDF and angular distribution. These changes could be used to identify the stress state of silicon nitride.

Acknowledgements. The authors would like to acknowledge the support of the Scientific Foundation for Start-up Scholars of Wenzhou University and the National Natural Science Foundation of China (50875115).

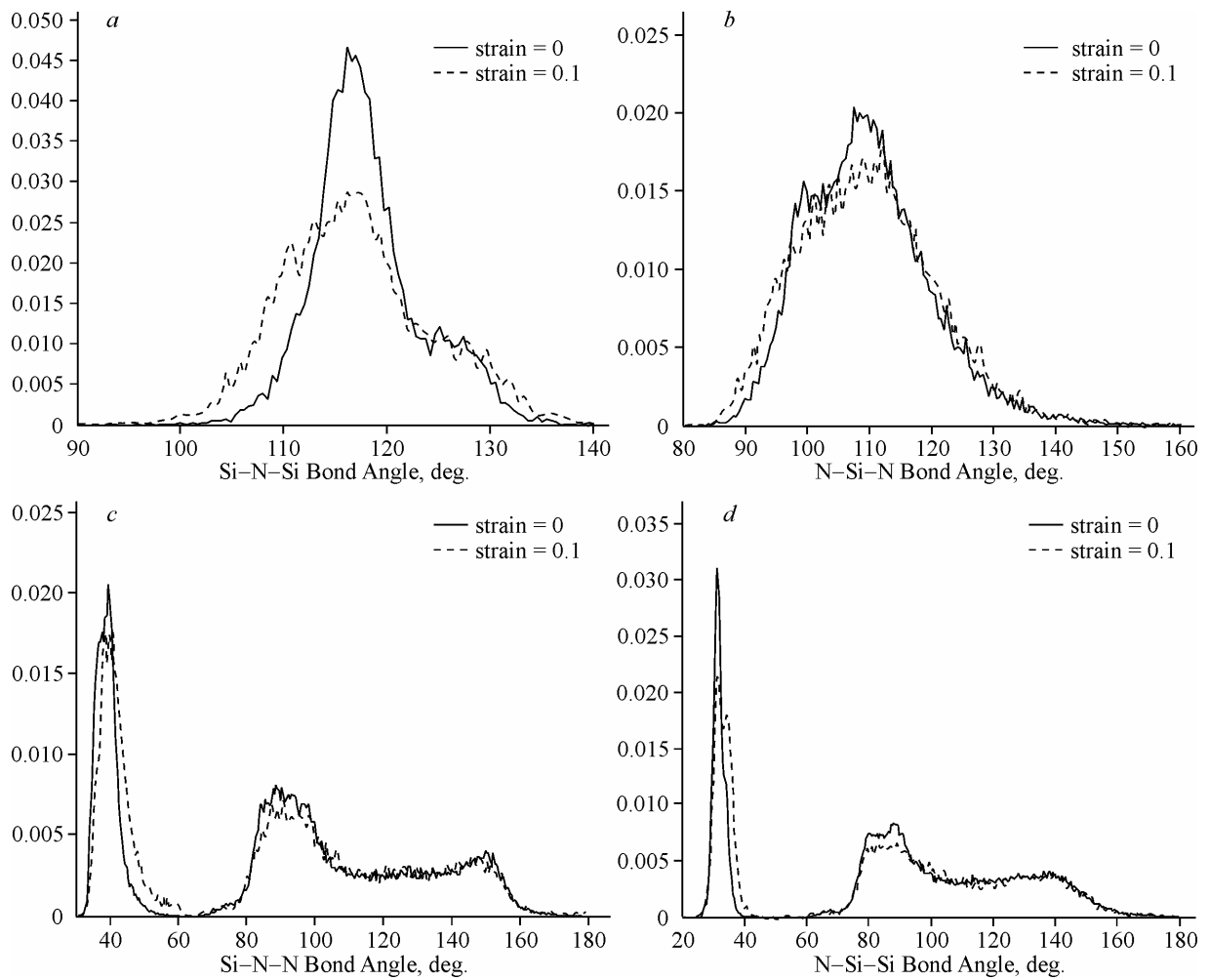


Fig. 4. Angular distributions of the Si_3N_4 structures

REFERENCES

1. Lattemann M., Ulrich S. // Surf. Coat. Technol. – 2007. – **201**, N 9-11. – P. 5564 – 5569.
2. Griffith A.A. // Philos. Trans. R. Soc. London, Ser. A. – 1921. – **221**. – P. 163 – 198.
3. Irwin D.R. // J. Appl. Mech. – 1957. – **24**, N 3. – P. 361 – 364.
4. Barenblatt G.I. // Adv. Appl. Mech. – 1962. – **7**. – P. 55 – 129.
5. Soules T.F., Busbey R.F. // J. Chem. Phys. – 1983. – **78**, N 10. – P. 6307 – 6317.
6. Swiler T.P., Varghese T., Simmons J.H. // J. Non-Cryst. Solids – 1995. – **181**, N 3. – P. 238 – 243.
7. Muralidharan K., Simmons J.H., Deymier P.A., Runge K. // J. Non-Cryst. Solids – 2005. – **351**, N 18. – P. 1532 – 1542.
8. Kalia R.K., Nakano A., Tsuruta K., Vashishta P. // Phys. Rev. Lett. – 1997. – **78**, N 4. – P. 689 – 692.
9. Tersoff J. // Physical Review B. – 1989. – **39**, N 8. – P. 55566 – 55568.
10. Mota F.D.B., Justo J.F., Fazio A. // Phys. Rev. B. – 1998. – **58**, N 13. – P. 8323 – 8328.
11. Resta N., Kohler C., Trebin H.R. // J. Amer. Ceram. Soc. – 2003. – **86**, N 8. – P. 1409 – 1414.
12. Matsunaga K., Iwamoto Y. // J. Amer. Ceram. Soc. – 2001. – **84**, N 10. – P. 2213 – 2219.
13. Plimpton S.J. // J. Comp. Phys. – 1995. – **117**, N 1. – P. 1 – 19.
14. Binder K., Kob W. Glassy Materials and Disordered Solids: an Introduction to Their Statistical Mechanics. – Singapore: World Scientific, 2005.
15. Aiyama T., Fukunaga T., Niihara K., Susuki K. // J. Non-Cryst. Solids – 1979. – **33**, N 2. – P. 133 – 139.
16. Misawa M., Fukingata T., Nihara K. et al. // J. Non-Cryst. Solids – 1979. – **34**, N 3. – P. 313 – 321.